Mixed formulation of finite elements based on the consistent couple stress theory

T. L. Chang

Department of Civil and Natural Resources Engineering, University of Canterbury, Christchurch, New Zealand, 8041.

Abstract

This work discusses the finite element formulation based on a six-field variational principle that incorporates the consistent couple stress theory. A simple, efficient, local iteration free solving procedure that covers both linear and nonlienar materials is derived. With proper interpolations, two example membrane elements are proposed. With the implemented elements, numerical experiments are conducted to investigate the performance of the in-plane drilling degrees of freedom introduced by the consistent couple stress theory.

Keywords: mixed formulation, couple stress theory, size dependence

1. Introduction

The Cauchy continuum mechanics has received wide recognition over the years and becomes the standard framework for many engineering disciplines. For simple, idealised problems, analytical solutions can be constructed [see, e.g., 1] with proper assumptions. The Cauchy theory also provides theoretical basis for the extensively used finite element methods. However, due to the lack of proper measure of rotation/curvature (and its force/stress conjugate), the Cauchy theory is incapable of describing the size effect, which is frequently seen in many materials at various scales (from nano to macro) and plays a vital role in fracture mechanics [2]. Besides, certain difficulties (e.g., kinematic compatibility among different types of elements) are encountered in problems involving elements with/without rotation field.

To overcome the shortcomings of the Cauchy theory, researchers have been investigating alternatives, which are often called nonlocal theories. A recent review [3] on relevant topics can be seen elsewhere. Among many different proposals, although disputed by others [4], the consistent couple stress theory [5] provides a promising framework by introducing curvature and couple stress vectors into the formulation. For further reviews on theoretical developments and experimental investigations regarding couple stress theory, interested authors can refer to the work by Pedgaonkar et al. [6] and the references therein.

Email address: tlcfem@gmail.com (T. L. Chang)

It is no doubt that in-plane rotations can be constructed within the Cauchy framework. Early attempts date back to the work by Allman [7]. Recent research work on membrane elements with in-plane drilling degrees of freedom can be seen in the review by Boutagouga [8]. However, the drilling degree of freedom defined within Cauchy theory shows significant size effect, which limits its application in modelling problems involving both membrane and beam elements [9]. In the couple stress theory, although the corresponding rigid body like rotation measures are defined as functions of translational displacements, by using the Lagrangian multiplier method, it is possible to interpolate rotation fields independently. This provides additional degrees of freedom which can be used to construct, for examples, shell and membrane elements with in-plane rotations. It would be interesting to investigate how the drilling degrees of freedom defined in the consistent couple stress theory would perform subjected to moment/rotation like loads and whether the associated size dependence could be alleviated.

This paper is organised as follows. The consistent couple stress theory is briefly reviewed by summarising key equations and quantities that are later used in finite element formulation. Based on this theory, a general mixed variational principle involving six independent fields are derived. After formulating system of linear equations, a simple, local iteration free solving strategy is designed for general nonlinear material models. Two membrane elements, named as couple stress triangle and quadrilateral, are implemented by choosing proper interpolations. With the proposed elements, the performance of the drilling degree of freedom is further investigated by conducting numerical experiments.

2. The Couple Stress Theory

Details of the adopted consistent couple stress theory can be seen elsewhere [5]. Here a brief summary of all necessary expressions utilised in finite element formulation is presented. No new contents are introduced in this section.

2.1. Kinematics

Within the infinitesimal strain framework, the couple stress theory [5] accounts for both symmetric and skew–symmetric parts of displacement gradient in kinematics, that is

$$\varepsilon_{ij} = \frac{1}{2}\left(u_{i,j} + u_{j,i}\right), \tag{1}$$

$$\omega_{ij} = \frac{1}{2}\left(u_{i,j} - u_{j,i}\right), \tag{2}$$

where u_i is the displacement field, ε_{ij} is the infinitesimal strain tensor, ω_{ij} is the skew–symmetric strain tensor that can be equivalently represented by the rotation vector θ_i,

$$\theta_i = \frac{1}{2}\epsilon_{ijk}\omega_{kj} = \frac{1}{2}\epsilon_{ijk}u_{k,j}, \tag{3}$$

where ϵ_{ijk} is the Levi–Civita (permutation) symbol. By utilising θ_i, the mean curvature vector κ_i is defined as

$$\kappa_i = \frac{1}{2}\epsilon_{ijk}\theta_{k,j}, \tag{4}$$

which can be further expressed in terms of u_i so that

$$\kappa_i = \frac{1}{4}\left(u_{j,ij} - u_{i,jj}\right). \tag{5}$$

The engineering mean curvature k_i can be defined accordingly to be

$$k_i = -2\kappa_i. \tag{6}$$

2.2. Equilibrium

The total stress tensor consists of two parts, namely the conventional symmetric stress tensor σ_{ij} and the additional skew–symmetric couple stress tensor μ_{ij}. Compared to the original literature [5], here a slightly different notation is used for brevity.

The couple stress vector μ_i dual to μ_{ij} can be defined as

$$\mu_{ji} = \epsilon_{ijk}\mu_k. \tag{7}$$

It is found that μ_i is the energetic conjugate to engineering mean curvature k_i.

The corresponding equilibrium equation can be shown as

$$\sigma_{ji,j} + \frac{1}{2}\left(\mu_{j,ij} - \mu_{i,jj}\right) + f_i = 0, \tag{8}$$

where f_i is the body force field.

2.3. Linear Elasticity

The stored energy function W can be defined as a function of ε_{ij} and κ_i such that

$$W\left(\varepsilon_{ij}, \kappa_i\right) = \frac{1}{2}\lambda\varepsilon_{ii}\varepsilon_{jj} + \mu\varepsilon_{ij}\varepsilon_{ij} + 8\eta\kappa_i\kappa_i, \tag{9}$$

where λ and μ are Lamé constants, η is the additional material constant. The corresponding constitutive relations for linear elasticity can then be derived to be

$$\mu_i = -8\eta\kappa_i = 4\eta k_i, \tag{10}$$

$$\sigma_{ij} = \lambda\delta_{ij}\varepsilon_{kk} + 2\mu\varepsilon_{ij}, \tag{11}$$

where δ_{ij} is the Kronecker delta. The additional constant η can be related to shear modulus μ by the characteristic length l according to the following expression,

$$\eta = l^2 \mu. \tag{12}$$

It is worth mentioning that l may not be a material constant and depends on geometry of structures [10]. Its determination is thus not further extended in this work.

Given that in this work σ_{ij} is assumed to be symmetric, without loss of generality, the variation of W can be expressed as

$$\delta W\left(\varepsilon_{ij}, \kappa_i\right) = \bar{\sigma}_{ij}\delta\varepsilon_{ij} - 2\bar{\mu}_i\delta\kappa_i, \tag{13}$$

or

$$\delta W\left(\varepsilon_{ij}, k_i\right) = \bar{\sigma}_{ij}\delta\varepsilon_{ij} + \bar{\mu}_i\delta k_i, \tag{14}$$

with $\bar{\sigma}_{ij}$ and $\bar{\mu}_i$ denoting stress and couple stress tensors obtained from typical strain driven constitutive model. For linear elasticity, they are simply

$$\bar{\sigma}_{ij} = \sigma_{ij}, \qquad \bar{\mu}_i = \mu_i.$$

2.4. Remarks

It could be noted that C^1 continuity is required by the displacement field u_i due to the presence of the second order derivatives in κ_i. Shape functions based on such as NURBS [see 11] that support C^1 continuity can be adopted to construct properly finite elements. Alternatively, θ_i can be treated as an independent field and the corresponding kinematic equations can be introduced into the functional via the method of Lagrangian multiplier, applications of which can be seen for example in the work by Pedgaonkar et al. [6], Darrall et al. [12], Deng and Dargush [13]. Further discussions of such a consistent couple stress theory can be also seen in the work by Hadjesfandiari and Dargush [14].

3. A Six–Field Mixed Framework

In this section, the variational theorem developed by Darrall et al. [12] is further extended to a more general form which resembles the Hu–Washizu variational theorem in the classic Cauchy theory.

By assuming the essential boundary conditions can be satisfied by proper construction, in absence of body force and surface force/moment traction, the total potential energy functional

over an arbitrary domain V can be simply expressed as

$$\Pi\left(\varepsilon_{ij},\kappa_i\right)=\int_V W\,\mathrm{d}V \tag{15}$$

where $W\left(\varepsilon_{ij},\kappa_i\right)$ is defined in Eq. (13) for linear elastic material. Since $\varepsilon_{ij}\left(u_i\right)$ and $\kappa_i\left(u_i\right)$ are functions of u_i, u_i is the only independent field in the above functional.

Now consider the case in which u_i, θ_i, ε_{ij}, and κ_i are all treated as independent fields, the kinematic equations Eq. (1), Eq. (4) and Eq. (3) need to be satisfied in a weak form. By introducing three Lagrangian multipliers α_{ij}, β_i and γ_i, those equations can be appended to the above functional so that

$$\begin{aligned}\Pi\left(u_i,\theta_i,\varepsilon_{ij},\kappa_i,\alpha_{ij},\beta_i,\gamma_i\right)=&\int_V W\,\mathrm{d}V+\int_V\alpha_{ij}\left(\varepsilon_{ij}-\frac{1}{2}\left(u_{i,j}+u_{j,i}\right)\right)\,\mathrm{d}V\\&+\int_V\beta_i\left(\kappa_i-\frac{1}{2}\epsilon_{ijk}\theta_{k,j}\right)\,\mathrm{d}V+\int_V\gamma_i\left(\theta_i-\frac{1}{2}\epsilon_{ijk}u_{k,j}\right)\,\mathrm{d}V.\end{aligned} \tag{16}$$

Taking the first variation leads to

$$\begin{aligned}\delta\Pi=&\int_V\bar{\sigma}_{ij}\delta\varepsilon_{ij}\,\mathrm{d}V-\int_V 2\bar{\mu}_i\delta\kappa_i\,\mathrm{d}V\\&+\int_V\delta\alpha_{ij}\left(\varepsilon_{ij}-\frac{1}{2}\left(u_{i,j}+u_{j,i}\right)\right)\,\mathrm{d}V+\int_V\alpha_{ij}\left(\delta\varepsilon_{ij}-\frac{1}{2}\left(\delta u_{i,j}+\delta u_{j,i}\right)\right)\,\mathrm{d}V\\&+\int_V\delta\beta_i\left(\kappa_i-\frac{1}{2}\epsilon_{ijk}\theta_{k,j}\right)\,\mathrm{d}V+\int_V\beta_i\left(\delta\kappa_i-\frac{1}{2}\epsilon_{ijk}\delta\theta_{k,j}\right)\,\mathrm{d}V\\&+\int_V\delta\gamma_i\left(\theta_i-\frac{1}{2}\epsilon_{ijk}u_{k,j}\right)\,\mathrm{d}V+\int_V\gamma_i\left(\delta\theta_i-\frac{1}{2}\epsilon_{ijk}\delta u_{k,j}\right)\,\mathrm{d}V.\end{aligned} \tag{17}$$

By performing integration by parts and applying the divergence theorem, one can find

$$-\frac{1}{2}\int_V\alpha_{ij}\left(\delta u_{i,j}+\delta u_{j,i}\right)\,\mathrm{d}V=\int_V\frac{\alpha_{ij,j}+\alpha_{ji,j}}{2}\delta u_i\,\mathrm{d}V-\int_S\frac{\alpha_{ij}+\alpha_{ji}}{2}n_j\delta u_i\,\mathrm{d}S, \tag{18}$$

$$-\frac{1}{2}\int_V\epsilon_{ijk}\beta_i\delta\theta_{k,j}\,\mathrm{d}V=\frac{1}{2}\int_V\epsilon_{ijk}\beta_{i,j}\delta\theta_k\,\mathrm{d}V-\frac{1}{2}\int_S\epsilon_{ijk}\beta_i n_j\delta\theta_k\,\mathrm{d}S, \tag{19}$$

$$-\frac{1}{2}\int_V\epsilon_{ijk}\gamma_i\delta u_{k,j}\,\mathrm{d}V=\frac{1}{2}\int_V\epsilon_{ijk}\gamma_{i,j}\delta u_k\,\mathrm{d}V-\frac{1}{2}\int_S\epsilon_{ijk}\gamma_i n_j\delta u_k\,\mathrm{d}S. \tag{20}$$

Here the boundary S is not further refined for simplicity.

Inserting the above expressions back to Eq. (17) gives

$$\begin{aligned}\delta\Pi = &\int_V \bar{\sigma}_{ij}\delta\varepsilon_{ij}\,\mathrm{d}V + \int_V \alpha_{ij}\delta\varepsilon_{ij}\,\mathrm{d}V - \int_V 2\bar{\mu}_i\delta\kappa_i\,\mathrm{d}V + \int_V \beta_i\delta\kappa_i\,\mathrm{d}V \\ &+ \int_V \delta\alpha_{ij}\left(\varepsilon_{ij} - \frac{1}{2}\left(u_{i,j}+u_{j,i}\right)\right)\,\mathrm{d}V + \int_V \delta\beta_i\left(\kappa_i - \frac{1}{2}\epsilon_{ijk}\theta_{k,j}\right)\,\mathrm{d}V \\ &+ \int_V \delta\gamma_i\left(\theta_i - \frac{1}{2}\epsilon_{ijk}u_{k,j}\right)\,\mathrm{d}V + \int_V \frac{\alpha_{ij,j}+\alpha_{ji,j}}{2}\delta u_i\,\mathrm{d}V + \frac{1}{2}\int_V \epsilon_{ijk}\gamma_{i,j}\delta u_k\,\mathrm{d}V \\ &+ \int_V \gamma_i\delta\theta_i\,\mathrm{d}V + \frac{1}{2}\int_V \epsilon_{ijk}\beta_{i,j}\delta\theta_k\,\mathrm{d}V - \frac{1}{2}\int_S \epsilon_{ijk}\beta_i n_j\delta\theta_k\,\mathrm{d}S \\ &- \int_S \frac{\alpha_{ij}+\alpha_{ji}}{2}n_j\delta u_i\,\mathrm{d}S - \frac{1}{2}\int_S \epsilon_{ijk}\gamma_i n_j\delta u_k\,\mathrm{d}S.\end{aligned} \tag{21}$$

Since the variations δu_i, $\delta\theta_i$, $\delta\varepsilon_{ij}$, $\delta\kappa_i$, $\delta\alpha_{ij}$, $\delta\beta_i$ and $\delta\gamma_i$ are arbitrary, the stationary condition requires the following equations involving Lagrangian multipliers to hold.

$$\bar{\sigma}_{ij} + \alpha_{ij} = 0, \quad -2\bar{\mu}_i + \beta_i = 0, \quad \alpha_{kj,j} + \alpha_{jk,j} + \epsilon_{ijk}\gamma_{i,j} = 0, \quad \gamma_k + \frac{1}{2}\epsilon_{ijk}\beta_{i,j} = 0. \tag{22}$$

It can be identified that $\alpha_{ij} = -\sigma_{ij}$, $\beta_i = 2\mu_i$ and $\gamma_i = \epsilon_{ijk}\mu_{k,j}$ with σ_{ij} and μ_i be independent fields. The third equation is essentially

$$0 = \left(\alpha_{kj} + \alpha_{jk}\right)_{,j} + \epsilon_{ijk}\epsilon_{imn}\mu_{m,nj} = \left(\alpha_{ji} + \alpha_{ij}\right)_{,j} + \left(\mu_{j,i} - \mu_{i,j}\right)_{,j},$$

which is the stress equilibrium Eq. (8) in absence of body force f_i.

The functional in its general form is then

$$\begin{aligned}\Pi\left(u_i, \theta_i, \varepsilon_{ij}, \sigma_{ij}, \kappa_i, \mu_i\right) = &\int_V W\,\mathrm{d}V - \int_V \sigma_{ij}\left(\varepsilon_{ij} - \frac{1}{2}\left(u_{i,j}+u_{j,i}\right)\right)\,\mathrm{d}V \\ &+ \int_V 2\mu_i\left(\kappa_i - \frac{1}{2}\epsilon_{ijk}\theta_{k,j}\right)\,\mathrm{d}V + \int_V \epsilon_{imn}\mu_{n,m}\left(\theta_i - \frac{1}{2}\epsilon_{ijk}u_{k,j}\right)\,\mathrm{d}V.\end{aligned} \tag{23}$$

It shall be noted that all boundary terms are omitted for brevity. In vector/matrix form, it can also be written as

$$\begin{aligned}\Pi\left(\boldsymbol{u}, \boldsymbol{\theta}, \boldsymbol{\varepsilon}, \boldsymbol{\sigma}, \boldsymbol{\kappa}, \boldsymbol{\mu}\right) = &\int_V W\,\mathrm{d}V + \int_V \boldsymbol{\sigma}^{\mathrm{T}}\left(\nabla^s\boldsymbol{u} - \boldsymbol{\varepsilon}\right)\,\mathrm{d}V \\ &+ \int_V 2\boldsymbol{\mu}^{\mathrm{T}}\left(\boldsymbol{\kappa} - \frac{1}{2}\nabla\times\boldsymbol{\theta}\right)\,\mathrm{d}V + \int_V \left(\nabla\times\boldsymbol{\mu}\right)^{\mathrm{T}}\left(\boldsymbol{\theta} - \frac{1}{2}\nabla\times\boldsymbol{u}\right)\,\mathrm{d}V.\end{aligned} \tag{24}$$

The symbol $\nabla^s\boldsymbol{u}$ is used to denote the result of $\left(u_{i,j}+u_{j,i}\right)/2$ expressed in Voigt form.

It occupies a form similar to that of the functional used in the Hu–Washizu principle. Fields $\boldsymbol{u}$, $\boldsymbol{\theta}$ and $\boldsymbol{\mu}$ require C^0 continuity, while $\boldsymbol{\kappa}$, $\boldsymbol{\varepsilon}$ and $\boldsymbol{\sigma}$ can be constant fields. Starting from Eq. (24), various levels of simplifications can be conducted to derive both mixed–type and hybrid–type

finite elements. For example, any of Eq. (1), Eq. (4) and Eq. (3) can be satisfied in strong forms thus the corresponding terms can be omitted from the functional. The mixed functional used by Darrall et al. [12], which is

$$\Pi\left(\boldsymbol{u},\boldsymbol{\theta},\boldsymbol{\mu}\right)=\int_V W\,\mathrm{d}V+\int_V\left(\nabla\times\boldsymbol{\mu}\right)^{\mathrm{T}}\left(\boldsymbol{\theta}-\frac{1}{2}\nabla\times\boldsymbol{u}\right)\,\mathrm{d}V+\Pi_{b.t.}. \tag{25}$$

can be obtained by enforcing Eq. (1) and Eq. (4) in strong forms. Besides, by considering Eq. (1) only, another functional can be obtained.

$$\begin{aligned}\Pi\left(\boldsymbol{u},\boldsymbol{\theta},\boldsymbol{\kappa},\boldsymbol{\mu}\right)=\int_V W\,\mathrm{d}V+\int_V 2\boldsymbol{\mu}^{\mathrm{T}}\left(\boldsymbol{\kappa}-\frac{1}{2}\nabla\times\boldsymbol{\theta}\right)\,\mathrm{d}V\\+\int_V\left(\nabla\times\boldsymbol{\mu}\right)^{\mathrm{T}}\left(\boldsymbol{\theta}-\frac{1}{2}\nabla\times\boldsymbol{u}\right)\,\mathrm{d}V+\Pi_{b.t.}.\end{aligned} \tag{26}$$

One can also apply divergence theorem to terms involving derivatives to convert between volume and surface integrals.

If, instead of $\boldsymbol{\kappa}$, engineering mean curvature $\boldsymbol{k}$ is used, an equivalent form can be derived following the same procedure.

$$\begin{aligned}\Pi\left(\boldsymbol{u},\boldsymbol{\theta},\boldsymbol{\varepsilon},\boldsymbol{\sigma},\boldsymbol{k},\boldsymbol{\mu}\right)=\int_V W\,\mathrm{d}V+\int_V\boldsymbol{\sigma}^{\mathrm{T}}\left(\nabla^s\boldsymbol{u}-\boldsymbol{\varepsilon}\right)\,\mathrm{d}V\\-\int_V\boldsymbol{\mu}^{\mathrm{T}}\left(\boldsymbol{k}+\nabla\times\boldsymbol{\theta}\right)\,\mathrm{d}V+\int_V\left(\nabla\times\boldsymbol{\mu}\right)^{\mathrm{T}}\left(\boldsymbol{\theta}-\frac{1}{2}\nabla\times\boldsymbol{u}\right)\,\mathrm{d}V.\end{aligned} \tag{27}$$

As can be predicted, the difference is solely the term $\int_V 2\boldsymbol{\mu}^{\mathrm{T}}\boldsymbol{\kappa}\,\mathrm{d}V=-\int_V\boldsymbol{\mu}^{\mathrm{T}}\boldsymbol{k}\,\mathrm{d}V$.

4. Finite Element Formulation

In this section, the linear equation system of the aforementioned general six–field variational principle Eq. (24) is derived. Since there is no other local residual apart from the one due to potential inelastic constitutive models, a locally iterative algorithm is not required. The final elemental stiffness may possess a form similar to that of conventional displacement based elements.

4.1. Linear System

Let six fields be discretized as follows.

$$\boldsymbol{u}=\boldsymbol{\phi}_u\boldsymbol{p},\quad\boldsymbol{\theta}=\boldsymbol{\phi}_\theta\boldsymbol{q},\quad\boldsymbol{\kappa}=\boldsymbol{\phi}_\kappa\boldsymbol{r},\quad\boldsymbol{\mu}=\boldsymbol{\phi}_\mu\boldsymbol{s},\quad\boldsymbol{\varepsilon}=\boldsymbol{\phi}_\varepsilon\boldsymbol{\beta},\quad\boldsymbol{\sigma}=\boldsymbol{\phi}_\sigma\boldsymbol{\alpha}. \tag{28}$$

Then, naturally, $\nabla^s \boldsymbol{u} = \boldsymbol{L}\boldsymbol{\phi}_u \boldsymbol{p}$ where $\boldsymbol{L}$ is the differential operator which can be expressed as

$$\boldsymbol{L} = \begin{bmatrix} \frac{\partial}{\partial x} & \cdot & \cdot & \frac{\partial}{\partial y} & \cdot & \frac{\partial}{\partial z} \\ \cdot & \frac{\partial}{\partial y} & \cdot & \frac{\partial}{\partial x} & \frac{\partial}{\partial z} & \cdot \\ \cdot & \cdot & \frac{\partial}{\partial z} & \cdot & \frac{\partial}{\partial y} & \frac{\partial}{\partial x} \end{bmatrix}^{\mathrm{T}} \tag{29}$$

in 3D space. Similarly, the curl operator can be expressed as $\frac{1}{2}\nabla \times (\cdot) = \boldsymbol{J}(\cdot)$ with

$$\boldsymbol{J} = \frac{1}{2}\begin{bmatrix} \cdot & -\frac{\partial}{\partial z} & \frac{\partial}{\partial y} \\ \frac{\partial}{\partial z} & \cdot & -\frac{\partial}{\partial x} \\ -\frac{\partial}{\partial y} & \frac{\partial}{\partial x} & \cdot \end{bmatrix}. \tag{30}$$

Now the functional can be rewritten as

$$\begin{aligned} \Pi(\boldsymbol{p}, \boldsymbol{q}, \boldsymbol{r}, \boldsymbol{s}, \boldsymbol{\beta}, \boldsymbol{\alpha}) = &\int_V W \,\mathrm{d}V + \int_V \boldsymbol{\alpha}^{\mathrm{T}} \boldsymbol{\phi}_\sigma^{\mathrm{T}} \left(\boldsymbol{L}\boldsymbol{\phi}_u \boldsymbol{p} - \boldsymbol{\phi}_\varepsilon \boldsymbol{\beta}\right) \,\mathrm{d}V \\ &+ \int_V 2\boldsymbol{s}^{\mathrm{T}} \boldsymbol{\phi}_\mu^{\mathrm{T}} \left(\boldsymbol{\phi}_\kappa \boldsymbol{r} - \boldsymbol{J}\boldsymbol{\phi}_\theta \boldsymbol{q}\right) \,\mathrm{d}V + \int_V 2\boldsymbol{s}^{\mathrm{T}} \left(\boldsymbol{J}\boldsymbol{\phi}_\mu\right)^{\mathrm{T}} \left(\boldsymbol{\phi}_\theta \boldsymbol{q} - \boldsymbol{J}\boldsymbol{\phi}_u \boldsymbol{p}\right) \,\mathrm{d}V. \end{aligned} \tag{31}$$

Taking variations leads to the following system of equations.

$$\begin{cases} \dfrac{\delta \Pi}{\delta \boldsymbol{p}} = \boldsymbol{0} \;\longrightarrow\; \displaystyle\int_V \left(\boldsymbol{L}\boldsymbol{\phi}_u\right)^{\mathrm{T}} \boldsymbol{\phi}_\sigma \boldsymbol{\alpha} - 2\left(\boldsymbol{J}\boldsymbol{\phi}_u\right)^{\mathrm{T}} \left(\boldsymbol{J}\boldsymbol{\phi}_\mu\right) \boldsymbol{s} \,\mathrm{d}V = \boldsymbol{R}_u, \\ \dfrac{\delta \Pi}{\delta \boldsymbol{q}} = \boldsymbol{0} \;\longrightarrow\; \displaystyle\int_V 2\left(\boldsymbol{\phi}_\theta^{\mathrm{T}} \boldsymbol{J}\boldsymbol{\phi}_\mu - \left(\boldsymbol{J}\boldsymbol{\phi}_\theta\right)^{\mathrm{T}} \boldsymbol{\phi}_\mu\right) \boldsymbol{s} \,\mathrm{d}V = \boldsymbol{R}_\theta, \\ \dfrac{\delta \Pi}{\delta \boldsymbol{r}} = \boldsymbol{0} \;\longrightarrow\; \displaystyle\int_V \boldsymbol{\phi}_\kappa^{\mathrm{T}} W_\kappa + 2\boldsymbol{\phi}_\kappa^{\mathrm{T}} \boldsymbol{\phi}_\mu \boldsymbol{s} \,\mathrm{d}V = \boldsymbol{0}, \\ \dfrac{\delta \Pi}{\delta \boldsymbol{s}} = \boldsymbol{0} \;\longrightarrow\; \displaystyle\int_V 2\left(\left(\boldsymbol{J}\boldsymbol{\phi}_\mu\right)^{\mathrm{T}} \boldsymbol{\phi}_\theta - \boldsymbol{\phi}_\mu^{\mathrm{T}} \boldsymbol{J}\boldsymbol{\phi}_\theta\right) \boldsymbol{q} + 2\boldsymbol{\phi}_\mu^{\mathrm{T}} \boldsymbol{\phi}_\kappa \boldsymbol{r} - 2\left(\boldsymbol{J}\boldsymbol{\phi}_\mu\right)^{\mathrm{T}} \boldsymbol{J}\boldsymbol{\phi}_u \boldsymbol{p} \,\mathrm{d}V = \boldsymbol{0}, \\ \dfrac{\delta \Pi}{\delta \boldsymbol{\beta}} = \boldsymbol{0} \;\longrightarrow\; \displaystyle\int_V \boldsymbol{\phi}_\varepsilon^{\mathrm{T}} W_\varepsilon \,\mathrm{d}V - \int_V \boldsymbol{\phi}_\varepsilon^{\mathrm{T}} \boldsymbol{\phi}_\sigma \boldsymbol{\alpha} \,\mathrm{d}V = \boldsymbol{0}, \\ \dfrac{\delta \Pi}{\delta \boldsymbol{\alpha}} = \boldsymbol{0} \;\longrightarrow\; \displaystyle\int_V \boldsymbol{\phi}_\sigma^{\mathrm{T}} \boldsymbol{L}\boldsymbol{\phi}_u \boldsymbol{p} - \boldsymbol{\phi}_\sigma^{\mathrm{T}} \boldsymbol{\phi}_\varepsilon \boldsymbol{\beta} \,\mathrm{d}V = \boldsymbol{0}. \end{cases} \tag{32}$$

In the above system, $\boldsymbol{R}_u$ and $\boldsymbol{R}_\theta$ are nodal forces/resistances due to omitted boundary terms, W_κ and W_ε denote the partial derivatives respectively.

By further denoting

$$\boldsymbol{E}_1 = \int_V \boldsymbol{\phi}_\varepsilon^{\mathrm{T}} \boldsymbol{C} \boldsymbol{\phi}_\varepsilon \,\mathrm{d}V, \quad \boldsymbol{E}_2 = \int_V \boldsymbol{\phi}_\kappa^{\mathrm{T}} \boldsymbol{D} \boldsymbol{\phi}_\kappa \,\mathrm{d}V, \quad \boldsymbol{H}_1 = -2 \int_V \left(\boldsymbol{J}\boldsymbol{\phi}_{\boldsymbol{u}}\right)^{\mathrm{T}} \left(\boldsymbol{J}\boldsymbol{\phi}_{\boldsymbol{\mu}}\right) \,\mathrm{d}V,$$
$$\boldsymbol{H}_2 = \int_V \left(\boldsymbol{L}\boldsymbol{\phi}_{\boldsymbol{u}}\right)^{\mathrm{T}} \boldsymbol{\phi}_{\boldsymbol{\sigma}} \,\mathrm{d}V, \quad \boldsymbol{H}_3 = 2 \int_V \boldsymbol{\phi}_{\boldsymbol{\theta}}^{\mathrm{T}} \boldsymbol{J}\boldsymbol{\phi}_{\boldsymbol{\mu}} - \left(\boldsymbol{J}\boldsymbol{\phi}_{\boldsymbol{\theta}}\right)^{\mathrm{T}} \boldsymbol{\phi}_{\boldsymbol{\mu}} \,\mathrm{d}V,$$
$$\boldsymbol{H}_4 = -2 \int_V \boldsymbol{\phi}_\kappa^{\mathrm{T}} \boldsymbol{\phi}_{\boldsymbol{\mu}} \,\mathrm{d}V, \quad \boldsymbol{H}_5 = \int_V \boldsymbol{\phi}_\varepsilon^{\mathrm{T}} \boldsymbol{\phi}_{\boldsymbol{\sigma}} \,\mathrm{d}V,$$

in which $\boldsymbol{C}$ and $\boldsymbol{D}$ denote material tangent moduli, the incremental form of linear system can be expressed as

$$\begin{bmatrix} \cdot & \cdot & \cdot & \boldsymbol{H}_1 & \cdot & \boldsymbol{H}_2 \\ \cdot & \cdot & \cdot & \boldsymbol{H}_3 & \cdot & \cdot \\ \cdot & \cdot & \boldsymbol{E}_2 & -\boldsymbol{H}_4 & \cdot & \cdot \\ \boldsymbol{H}_1^{\mathrm{T}} & \boldsymbol{H}_3^{\mathrm{T}} & -\boldsymbol{H}_4^{\mathrm{T}} & \cdot & \cdot & \cdot \\ \cdot & \cdot & \cdot & \cdot & \boldsymbol{E}_1 & -\boldsymbol{H}_5 \\ \boldsymbol{H}_2^{\mathrm{T}} & \cdot & \cdot & \cdot & -\boldsymbol{H}_5^{\mathrm{T}} & \cdot \end{bmatrix} \begin{bmatrix} \Delta\boldsymbol{p} \\ \Delta\boldsymbol{q} \\ \Delta\boldsymbol{r} \\ \Delta\boldsymbol{s} \\ \Delta\boldsymbol{\beta} \\ \Delta\boldsymbol{\alpha} \end{bmatrix} = \boldsymbol{R}. \tag{33}$$

In which, $\boldsymbol{R}$ is used to denote residual whose discrete form is not shown. As can be seen later, it is possible to compute resistance directly based on Eq. (32).

4.2. Solution Procedure

4.2.1. Option One — Invertible $\boldsymbol{E}_1$ and $\boldsymbol{E}_2$

Since $\boldsymbol{E}_1$ and $\boldsymbol{E}_2$ are guaranteed to be square matrices, typically they are invertible with sufficient integration points provided, performing static condensation leads to the following elemental stiffness.

$$\boldsymbol{K} = \begin{bmatrix} \boldsymbol{H}_2 \left(\boldsymbol{H}_5^{\mathrm{T}} \boldsymbol{E}_1^{-1} \boldsymbol{H}_5\right)^{-1} \boldsymbol{H}_2^{\mathrm{T}} + \boldsymbol{H}_1 \left(\boldsymbol{H}_4^{\mathrm{T}} \boldsymbol{E}_2^{-1} \boldsymbol{H}_4\right)^{-1} \boldsymbol{H}_1^{\mathrm{T}} & \boldsymbol{H}_1 \left(\boldsymbol{H}_4^{\mathrm{T}} \boldsymbol{E}_2^{-1} \boldsymbol{H}_4\right)^{-1} \boldsymbol{H}_3^{\mathrm{T}} \\ \boldsymbol{H}_3 \left(\boldsymbol{H}_4^{\mathrm{T}} \boldsymbol{E}_2^{-1} \boldsymbol{H}_4\right)^{-1} \boldsymbol{H}_1^{\mathrm{T}} & \boldsymbol{H}_3 \left(\boldsymbol{H}_4^{\mathrm{T}} \boldsymbol{E}_2^{-1} \boldsymbol{H}_4\right)^{-1} \boldsymbol{H}_3^{\mathrm{T}} \end{bmatrix}. \tag{34}$$

The above procedure requires matrix inversions to be conducted at element level whenever tangent moduli update. This is considered not very efficient for nonlinear analysis.

Stability Condition. Let the size of $\boldsymbol{\phi}_\varepsilon$ be $i \times j$ and the size of $\boldsymbol{\phi}_\sigma$ be $i \times k$, then the number of integration points n_{ip} must satisfy the following inequality for $\boldsymbol{E}_1$ to be invertible,

$$n_{ip} \cdot \min\left(i,\, j\right) \geqslant \max\left(i,\, j\right). \tag{35}$$

Furthermore, for $\boldsymbol{H}_5^{\mathrm{T}}\boldsymbol{E}_1^{-1}\boldsymbol{H}_5$ to be invertible,

$$n_{ip}\cdot\min\left(i,\ j,\ k\right)\geqslant\max\left(i,\ j,\ k\right). \tag{36}$$

This, however, only guarantees successful computation of elemental stiffness matrix thus is the minimum condition. Denoting the number of rigid body motion as n_f and the size of elemental stiffness matrix as n_k, then for a single element, at least

$$n_{ip}\cdot\min\left(i,\ j,\ k\right)\geqslant n_k-n_f. \tag{37}$$

Similar procedure can be applied to term $\boldsymbol{H}_4^{\mathrm{T}}\boldsymbol{E}_2^{-1}\boldsymbol{H}_4$. Let the size of $\boldsymbol{\phi}_{\boldsymbol{\kappa}}$ be $l\times m$ and the size of $\boldsymbol{\phi}_{\boldsymbol{\mu}}$ be $l\times n$, then

$$n_{ip}\cdot\min\left(l,\ m,\ n\right)\geqslant\max\left(l,\ m,\ n,\ n_k-n_f\right). \tag{38}$$

Eventually,

$$n_{ip}\cdot\min\left(i,\ j,\ k,\ l,\ m,\ n\right)\geqslant\max\left(i,\ j,\ k,\ l,\ m,\ n,\ n_k-n_f\right). \tag{39}$$

4.2.2. Option Two — Invertible $\boldsymbol{H}_4$ and $\boldsymbol{H}_5$

By proper construction, $\boldsymbol{H}_4$ and $\boldsymbol{H}_5$ can be square and invertible. Similar to the work by the author [15], by static condensation, one can obtain

$$\begin{bmatrix}\boldsymbol{H}_2\boldsymbol{H}_5^{-1}\boldsymbol{E}_1\boldsymbol{H}_5^{-\mathrm{T}}\boldsymbol{H}_2^{\mathrm{T}}+\boldsymbol{H}_1\boldsymbol{H}_4^{-1}\boldsymbol{E}_2\boldsymbol{H}_4^{-\mathrm{T}}\boldsymbol{H}_1^{\mathrm{T}} & \boldsymbol{H}_1\boldsymbol{H}_4^{-1}\boldsymbol{E}_2\boldsymbol{H}_4^{-\mathrm{T}}\boldsymbol{H}_3^{\mathrm{T}}\\ \boldsymbol{H}_3\boldsymbol{H}_4^{-1}\boldsymbol{E}_2\boldsymbol{H}_4^{-\mathrm{T}}\boldsymbol{H}_1^{\mathrm{T}} & \boldsymbol{H}_3\boldsymbol{H}_4^{-1}\boldsymbol{E}_2\boldsymbol{H}_4^{-\mathrm{T}}\boldsymbol{H}_3^{\mathrm{T}}\end{bmatrix}\begin{bmatrix}\Delta\boldsymbol{p}\\ \Delta\boldsymbol{q}\end{bmatrix}=\boldsymbol{R}. \tag{40}$$

The above system can be conveniently converted into a more expressive form, in which the elemental stiffness matrix $\boldsymbol{K}$ can be shown as

$$\boldsymbol{K}=\boldsymbol{K}_1+\boldsymbol{K}_2 \tag{41}$$

with

$$\boldsymbol{K}_1=\begin{bmatrix}\boldsymbol{H}_2\boldsymbol{H}_5^{-1} & \cdot\\ \cdot & \cdot\end{bmatrix}\begin{bmatrix}\boldsymbol{E}_1 & \cdot\\ \cdot & \cdot\end{bmatrix}\begin{bmatrix}\boldsymbol{H}_5^{-\mathrm{T}}\boldsymbol{H}_2^{\mathrm{T}} & \cdot\\ \cdot & \cdot\end{bmatrix}, \tag{42}$$

$$\boldsymbol{K}_2=\begin{bmatrix}\cdot & \boldsymbol{H}_1\boldsymbol{H}_4^{-1}\\ \cdot & \boldsymbol{H}_3\boldsymbol{H}_4^{-1}\end{bmatrix}\begin{bmatrix}\cdot & \cdot\\ \cdot & \boldsymbol{E}_2\end{bmatrix}\begin{bmatrix}\cdot & \cdot\\ \boldsymbol{H}_4^{-\mathrm{T}}\boldsymbol{H}_1^{\mathrm{T}} & \boldsymbol{H}_4^{-\mathrm{T}}\boldsymbol{H}_3^{\mathrm{T}}\end{bmatrix}. \tag{43}$$

The first term $\boldsymbol{K}_1$ solely depends on conventional displacement, strain and stress as defined in the Cauchy theory. Thus it can be derived from the Hu–Washizu theorem.

Since all $\boldsymbol{H}_n$ matrices are constant once interpolations are determined, they only need to be

computed once during the initialisation stage. Furthermore, $\boldsymbol{H}_n$ require no additional storage as $\boldsymbol{H}_2\boldsymbol{H}_5^{-1}\boldsymbol{\phi}_{\boldsymbol{\varepsilon}}^{\mathrm{T}}$, $\boldsymbol{H}_1\boldsymbol{H}_4^{-1}\boldsymbol{\phi}_{\boldsymbol{\kappa}}^{\mathrm{T}}$ and $\boldsymbol{H}_3\boldsymbol{H}_4^{-1}\boldsymbol{\phi}_{\boldsymbol{\kappa}}^{\mathrm{T}}$ can be stored as 'equivalent strain matrices' for each integration point. Once the elemental stiffness matrix is computed, reordering of degrees of freedom may be performed.

It can be noted that the elemental stiffness possesses a symmetric structure although moduli $\boldsymbol{E}_1$ and $\boldsymbol{E}_2$ may be asymmetric due to for example non-associative plasticity in the case of material nonlinearity.

Stability Condition. This option only requires the inversion of square matrices $\boldsymbol{H}_4$ and $\boldsymbol{H}_5$. Thus $\boldsymbol{\phi}_{\boldsymbol{\varepsilon}}$ ($\boldsymbol{\phi}_{\boldsymbol{\kappa}}$) and $\boldsymbol{\phi}_{\boldsymbol{\sigma}}$ ($\boldsymbol{\phi}_{\boldsymbol{\mu}}$) have the same size. Let $i \times j$ be the size of $\boldsymbol{\phi}_{\boldsymbol{\varepsilon}}$ and $m \times n$ be the size of $\boldsymbol{\phi}_{\boldsymbol{\kappa}}$, then the stability condition becomes

$$n_{ip} \cdot \min\left(i,\ j,\ m,\ n\right) \geqslant \max\left(i,\ j,\ m,\ n,\ n_k - n_f\right). \tag{44}$$

4.2.3. Resistance

From the third equation of the stationary condition Eq. (32), $\boldsymbol{s}$ solely depends on material response thus can be computed directly as

$$\boldsymbol{s} = \boldsymbol{H}_4^{-1} \int_V \boldsymbol{\phi}_{\boldsymbol{\kappa}}^{\mathrm{T}} \bar{\boldsymbol{\mu}}\, \mathrm{d}V. \tag{45}$$

Applying the same strategy to the fifth equation, one can obtain

$$\boldsymbol{\alpha} = \boldsymbol{H}_5^{-1} \int_V \boldsymbol{\phi}_{\boldsymbol{\varepsilon}}^{\mathrm{T}} \bar{\boldsymbol{\sigma}}\, \mathrm{d}V. \tag{46}$$

In the above equations, similar to Eq. (13), $\bar{\boldsymbol{\sigma}}$ and $\bar{\boldsymbol{\mu}}$ denote the stress and couple stress obtained from material model. Inserting Eq. (45) and Eq. (46) back to the first two equations in Eq. (32), one can obtain the elemental resistance as

$$\begin{bmatrix} \boldsymbol{R}_{\boldsymbol{u}} \\ \boldsymbol{R}_{\boldsymbol{\theta}} \end{bmatrix} = \begin{bmatrix} \boldsymbol{H}_2\boldsymbol{H}_4^{-1} \int_V \boldsymbol{\phi}_{\boldsymbol{\kappa}}^{\mathrm{T}} \bar{\boldsymbol{\mu}}\, \mathrm{d}V + \boldsymbol{H}_1\boldsymbol{H}_5^{-1} \int_V \boldsymbol{\phi}_{\boldsymbol{\varepsilon}}^{\mathrm{T}} \bar{\boldsymbol{\sigma}}\, \mathrm{d}V \\ \boldsymbol{H}_3\boldsymbol{H}_4^{-1} \int_V \boldsymbol{\phi}_{\boldsymbol{\kappa}}^{\mathrm{T}} \bar{\boldsymbol{\mu}}\, \mathrm{d}V \end{bmatrix}. \tag{47}$$

One material response is computed, elemental resistance can be conveniently assembled without worrying about local residual.

4.2.4. Remarks

Although the second option appears to be more efficient and possesses a form similar to that of displacement based elements, both options can be chosen to formulate elemental stiffness matrix and they share similar stability conditions. However, they may require different numbers of shape functions for the corresponding fields in order to construct square matrices. Depending on the

type of element and the number of available integration points, one may switch from one option to another for optimal formulation.

If Eq. (27) is used, expect for replacing all $\boldsymbol{\phi}_{\boldsymbol{\kappa}}$ with $\boldsymbol{\phi}_{\boldsymbol{k}}$, only $\boldsymbol{H}_4$ needs to be modified.

$$\boldsymbol{H}_4 = \int_V \boldsymbol{\phi}_{\boldsymbol{k}}^{\mathrm{T}} \boldsymbol{\phi}_{\boldsymbol{\mu}} \, \mathrm{d}V, \tag{48}$$

where $\boldsymbol{\phi}_{\boldsymbol{k}}$ is the interpolation of engineering mean curvature $\boldsymbol{k}$.

4.3. Some Basic Elements

Since the incremental form and elemental stiffness are given in Eq. (33) and Eq. (41), there is no difficulty in constructing various types of elements such as serendipity quadrilaterals with various nodes, axisymmetric triangle/quadrilateral, eight-node brick/cube, four-node tetrahedron and higher order elements. The procedure follows a standard FEM approach. Two elements named as couple stress triangle and quadrilateral (CSMT3 and CSMQ4) are formulated as examples. Other elements implemented [16] include: three-node second order triangle (CSMT6), serendipity quadrilaterals with five to eight nodes (CSMQ5, CSMQ6, CSMQ7, CSMQ8).

4.3.1. An Elementary Membrane Element — CSMT3

Not all couple stress theories support membrane problems, the popular modified couple stress theory [17] adopts a symmetric couple stress tensor, with which in-plane response cannot be fully decoupled from out-of-plane response. Discussions of relevant topics can be seen elsewhere [14]. The consistent couple stress theory is free from similar issues, which makes it more appealing for a wide range of general continuum problems.

The simplest membrane element may be the three-node triangular element. For plane stress problem, given the constitutive equation between mean curvature vector κ_i and couple stress vector μ_i occupies the form shown in Eq. (10), it is clear that in-plane and out-of-plane actions are decoupled. Thus six fields reduce to the following Voigt forms.

$$\boldsymbol{u} = \begin{bmatrix} u_x \\ u_y \end{bmatrix}, \quad \boldsymbol{\theta} = \begin{bmatrix} \theta_z \end{bmatrix}, \quad \boldsymbol{\kappa} = \begin{bmatrix} \kappa_x \\ \kappa_y \end{bmatrix}, \quad \boldsymbol{\mu} = \begin{bmatrix} \mu_x \\ \mu_y \end{bmatrix}, \quad \boldsymbol{\varepsilon} = \begin{bmatrix} \varepsilon_x \\ \varepsilon_y \\ \gamma_{xy} \end{bmatrix}, \quad \boldsymbol{\sigma} = \begin{bmatrix} \sigma_x \\ \sigma_y \\ \tau_{xy} \end{bmatrix}. \tag{49}$$

The linear mapping is used for coordinate, displacement, drilling rotation and couple stress, that is

$$\chi = \sum_{i=1}^{3} N_i \chi_i \tag{50}$$

where N_i is the complete first order shape function with modes $\begin{bmatrix} 1 & x & y \end{bmatrix}$, χ represents any of x, y, u_x, u_y, θ_z, κ_x, κ_y, μ_x and μ_y. Thus for each fields, three nodal values are used for interpolation.

Given that $\boldsymbol{u}$ is linearly interpolated, $\boldsymbol{\varepsilon}$ and $\boldsymbol{\sigma}$ can be chosen to be constant fields.

$$\boldsymbol{\varepsilon} = \begin{bmatrix} 1 & \cdot & \cdot \\ \cdot & 1 & \cdot \\ \cdot & \cdot & 1 \end{bmatrix} \begin{bmatrix} \beta_1 \\ \beta_2 \\ \beta_3 \end{bmatrix}, \qquad \boldsymbol{\sigma} = \begin{bmatrix} 1 & \cdot & \cdot \\ \cdot & 1 & \cdot \\ \cdot & \cdot & 1 \end{bmatrix} \begin{bmatrix} \alpha_1 \\ \alpha_2 \\ \alpha_3 \end{bmatrix}. \tag{51}$$

In this case, β_i and α_i are essentially strain and stress components.

The explicit forms are not listed here for brevity. Interested readers are referred to typical textbooks on finite element methods for details of formulating interpolation matrices [see, e.g., 18, section 5.1.3.1]. Three integration points are used for numerical integration. This element is denoted as couple stress mixed triangle (CSMT3) element.

The CSMT3 element is essentially an extension of constant strain triangle (CST) element (CPS3 and CPE3 in ABAQUS notion) with additional fields incorporates mean curvature and couple stress. Given that only linear and constant interpolations are used, its performance shall be similar to that of CST.

4.3.2. A Four-Node Quadrilateral Membrane Element — CSMQ4

Similarly, the aforementioned formulation can be applied to four-node quadrilaterals. The standard isoparametric mapping can be applied.

$$\chi = \sum_{i=1}^{4} N_i \chi_i \tag{52}$$

with $N_i = (1 + \xi_i \xi)(1 + \eta_i \eta)/4$ where ξ and η are parent coordinates while ξ_i and η_i are values of parent coordinates of target node. Again, χ can be any of x, y, u_x, u_y, θ_z, κ_x, κ_y, μ_x and μ_y. A complete first order interpolation can be chosen for both strain and stress.

$$\boldsymbol{\phi}_{\boldsymbol{\varepsilon}} = \boldsymbol{\phi}_{\boldsymbol{\sigma}} = \begin{bmatrix} 1 & \cdot & \cdot & \cdot & y & \cdot & x \\ \cdot & 1 & \cdot & x & \cdot & y & \cdot \\ \cdot & \cdot & 1 & \cdot & \cdot & -x & -y \end{bmatrix}. \tag{53}$$

It shall be mentioned that the stress defined above satisfies the Airy stress function, however, in the consistent couple stress theory, $\boldsymbol{\sigma}$ is not only governed by the Airy stress function but also an additional stress function [5] from which $\boldsymbol{\mu}$ can be derived. Based on previous discovery [15], $\boldsymbol{\phi}_{\boldsymbol{\varepsilon}}$ can be further modified to include the Poisson effect, which overcomes (near) incompressible problems. A 2×2 Gauss quadrature is used for numerical integration, this element is denoted as couple stress mixed quadrilateral (CSMQ4) element.

Given that the displacement interpolation only uses four modes $\begin{bmatrix} 1 & x & y & xy \end{bmatrix}$, one can further define internal degrees of freedom to complete the second order interpolation so that performance can be improved.

5. Numerical Examples

Given that some preliminary results have been given by Pedgaonkar et al. [6], Darrall et al. [12], we focus on the performance of drilling degrees of freedom offered by the consistent couple stress theory and the objectivity of the corresponding numerical results in this work.

5.1. Patch Test

As a convention, the classic constant strain patch test defines four elements in a rectangular panel as shown in Fig. 1 is firstly presented. The linear displacement field can be successfully

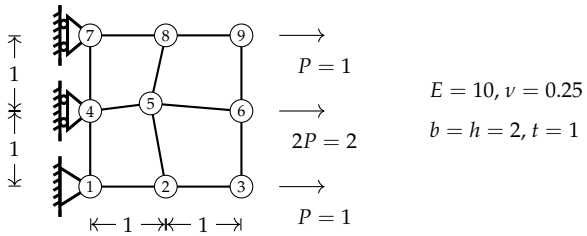

Figure 1: constant strain patch test

computed by using CSMQ4 elements with arbitrary location of the middle node.

Since strain field remains constant, no couple stress would be generated in this example. As the result, whether nodal rotations are constrained has no impact on final results. Due to the same reason, any positive numbers can be chosen as the characteristic length l.

5.2. Plane Ring

For the purpose of validation of implemented elements, the plane ring example is modeled. The analytical solution can be seen elsewhere [5]. The ring shown in Fig. 2 is subjected to plane strain condition with inner radius $r_1 = 1$, outer radius $r_2 = 2$, shear modulus $\mu = 1$ and Poisson's ratio $\nu = 0.4$. The outer boundary is fixed thus translation is zero. A uniform horizontal

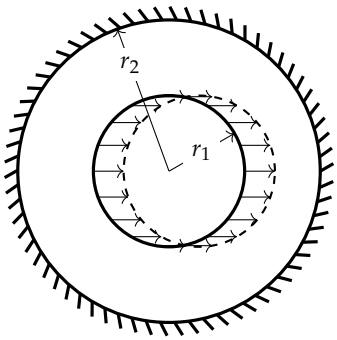

Figure 2: plane ring subjected to uniform horizontal displacement

displacement is applied to the inner boundary while the vertical displacement is constrained. As

free couple traction is assumed on both boundaries, the corresponding rotation is not necessarily zero. Due to symmetry, the finite element model defines the geometry of half of the ring with a structured grid of size 25×100. Three elements are tested: CSMT3, CSMQ4 and CSMQ8. The deformed model can be seen in Fig. 3.

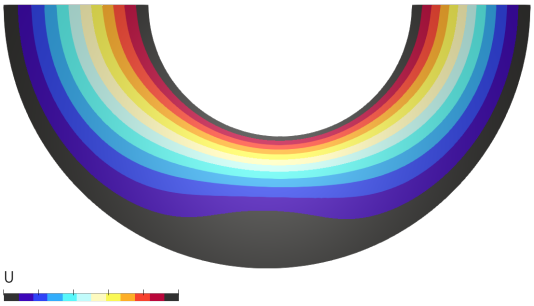

Figure 3: deformed half ring model with $l = 0.1$

Numerical results of the transverse displacement u_θ along the vertical center line are presented in Fig. 4 with analytical solution obtained by using proper l. The numerical solution matches the analytical one well, indicating the implementation is correct. Since no dedicated optimisation is designed to improve the performance apart from the mixed formulation, relatively dense mesh grids are required to reduce error. The second order quadrilateral CSMQ8 shows higher accuracy as can be predicted based on experience with the Cauchy framework.

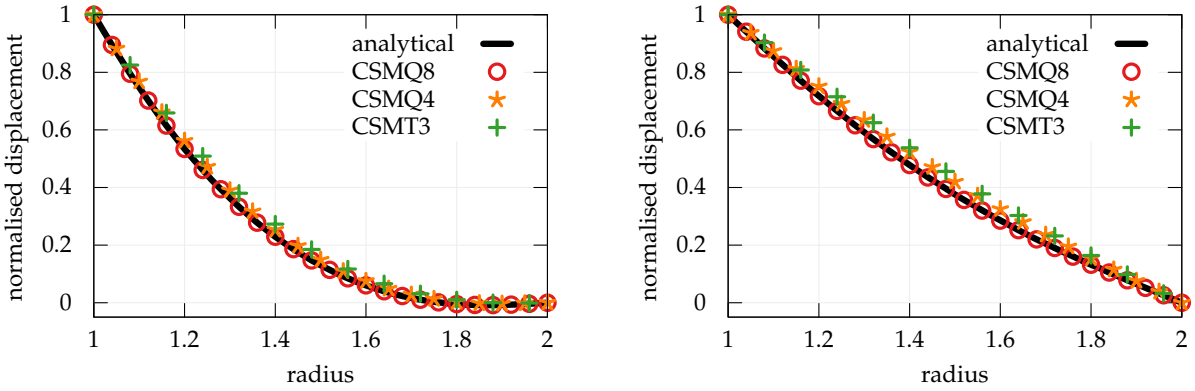

(a) $l = 0.1$ (b) $l = 0.5$

Figure 4: u_θ at vertical center line

5.3. *Membrane–Beam Joint*

From the previous two examples, it can be concluded that the formulation developed in this work and the corresponding implementation are both correct. Since the drilling degree of freedom defined in the consistent couple stress theory has an energetic conjugate — curl of couple stress

$\nabla \times \boldsymbol{\mu}$ as can be seen in Eq. (27), size dependence can be successfully captured by its nature. In this example, the performance of drilling DoFs is investigated. Although it is possible to directly apply loads to drilling DoFs as 'moments', a membrane–beam joint, which is frequently encountered in structural engineering, is used instead.

The model shown in Fig. 5 is subjected to plane stress condition and consists of a square panel of size 10×10 and a beam of length 4. The height of beam section is 1 while the thickness along z-axis is chosen to be unity. A unit displacement is applied to the free end of beam and the cor-

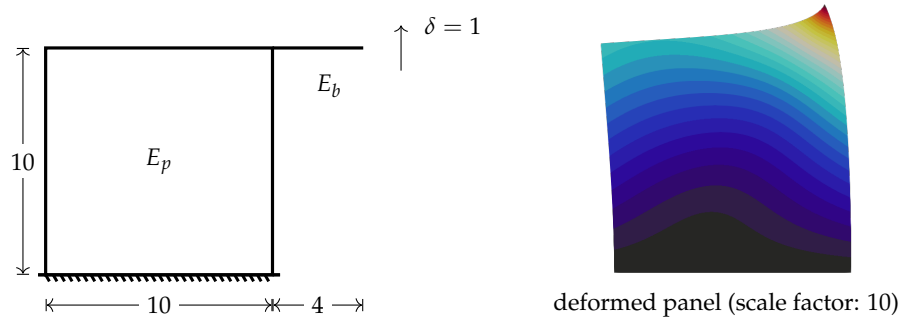

Figure 5: panel joint with attached beam

responding resistance is recorded for comparison. The panel is modelled by a structured grid of with various numbers of membrane elements (SGCMQG [9] and CSMQ4) along each direction while the beam is modelled by an elastic Euler–Bernoulli beam. Nodal rotations formulated within the Cauchy theory exhibit significant size dependency. Here, SGCMQ element is used as a reference. A mixed action (rotation and translation) is experienced by the panel.

Three pairs of panel and beam elastic moduli are chosen to represent different deformation patterns. The analysis is performed with characteristic length l ranging from 10^3 to 10^{-3}. Numerical results are presented in Fig. 6. The following observations can be made.

1. When either l or E_p/E_b is large, the panel is sufficiently rigid so that deformation is mainly contributed by the beam, resulting in a cantilever like structure, the corresponding resistance is close to the upper bound 3.906 3 computed via a cantilever model.
2. For Cauchy theory based elements, the corresponding rotational stiffness decreases (thus deformation localises) with refined meshes. On the contrary, CSMQ4 is less sensitive to mesh sizes. With fixed l, the variation of resistance generated by CSMQ4 is significantly smaller than that of SGCMQG.
3. With GCMQ4, mesh refinement has the most noticeable impact on numerical results when $l = 0.1$ to 1.

It can be further inferred that with sufficient number of elements, both SGCMQG and CSMQ4 with a small l would converge to the same solution in which deformation is localised in a small region around the top right corner.

Given that GCMQ elements can converge to analytical solutions as can be seen in the previous example, it is no doubt that the consistent couple stress theory provides an appealing (and maybe more realistic) approach when it comes to similar problems involving in-plane rotations.

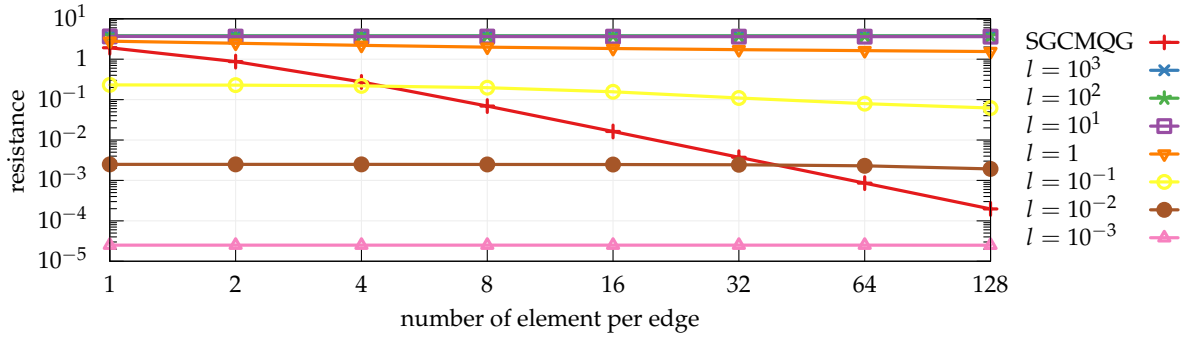

(a) $E_p/E_b = 0.1$

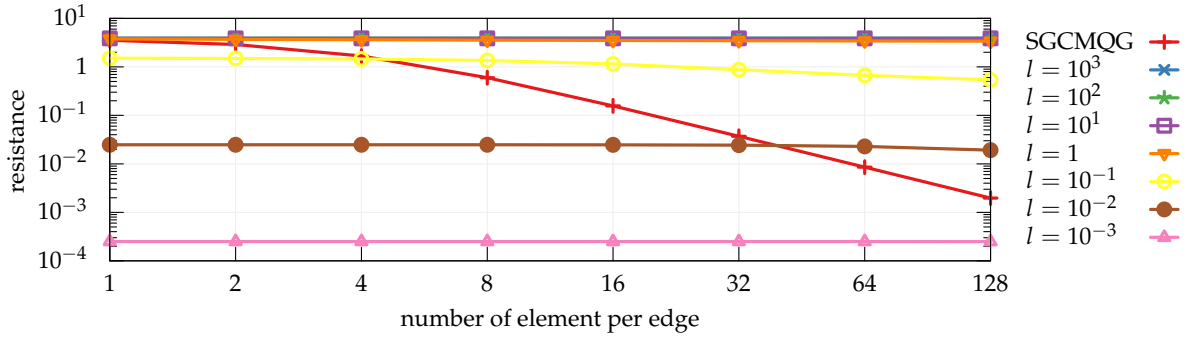

(b) $E_p/E_b = 1$

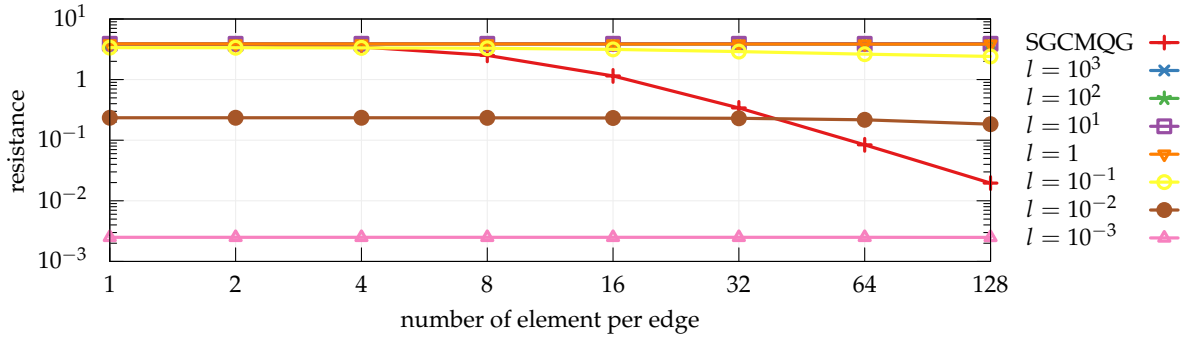

(c) $E_p/E_b = 10$

Figure 6: beam end resistance subjected to unit vertical displacement

However, the determination of characteristic length l could be a challenge task. The corresponding experimental theories shall be investigated in future. With properly defined l, it is believed that the implemented couple stress elements can model in-plane rotation with acceptable accuracy. As discussed by others [e.g., 12], a large l would suppress bending action, resulting in a shear dominated deformation pattern.

5.4. Inelastic Response

Noting that in Eq. (9) the stored energy function can be split into two parts and each is independent from the other, it would be interesting to investigate whether objective results can be obtained for softening response with the assist of couple stress.

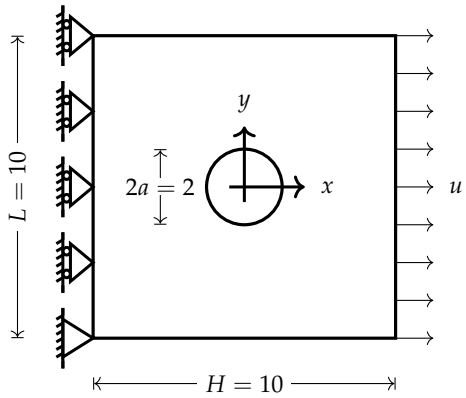

Figure 7: square plate with circular hole

In this example, it is simply assumed that the couple part of W remains 'elastic' so that η is a constant. The uniform extension of a square plate with a hole of unit radius, depicted in Fig. 7, subjected to plane stress condition is simulated with a softening isotropic J2 plasticity model. The following material parameters are chosen: elastic modulus $E = 1\,000$, Poisson's ratio $\nu = 0.2$, yield stress $\sigma_y = 1$, hardening ratio $b = -0.03$. The thickness t is set to unity.

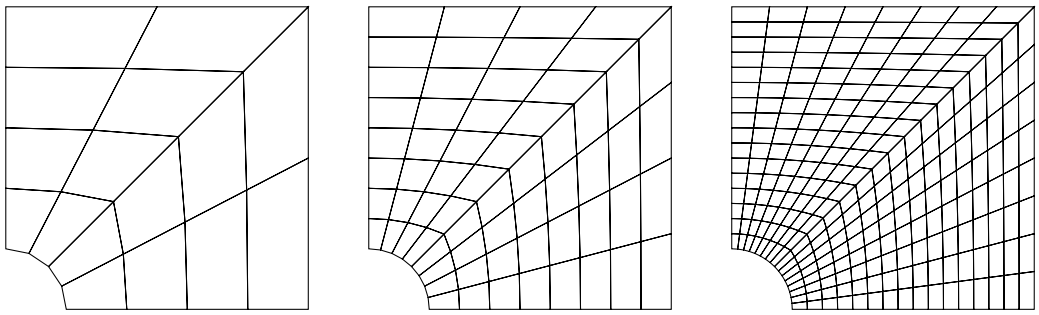

Figure 8: a quarter of plane simulated with three different meshes

6. Conclusions

In this work, based on the consistent couple stress theory, a mixed variational theorem is developed with six independent fields. Finite elements of various types can be formulated accordingly for problems with both linear and nonlinear materials, although it is still difficult to further investigate the performance of the couple stress theory beyond elasticity for the moment, given

that most existing constitutive models are developed based on the Cauchy theory. It would be interesting to see work in that regard in future.

The proposed elements have been implemented in `suanPan` [16]. Sample model scripts can be found online[1].

References

[1] S. Timoshenko, Theory of elasticity, 3rd ed., McGraw-Hill Education, New Delhi, India, 2010.

[2] Z. P. Bažant, Size effect in blunt fracture: Concrete, rock, metal, Journal of Engineering Mechanics 110 (1984) 518–535. doi:10.1061/(asce)0733-9399(1984)110:4(518).

[3] M. Shaat, E. Ghavanloo, S. A. Fazelzadeh, Review on nonlocal continuum mechanics: Physics, material applicability, and mathematics, Mechanics of Materials 150 (2020) 103587. doi:10.1016/j.mechmat.2020.103587.

[4] P. Neff, I. Münch, I.-D. Ghiba, A. Madeo, On some fundamental misunderstandings in the indeterminate couple stress model. a comment on recent papers of A.R. Hadjesfandiari and G.F. Dargush, International Journal of Solids and Structures 81 (2016) 233–243. doi:10.1016/j.ijsolstr.2015.11.028.

[5] A. R. Hadjesfandiari, G. F. Dargush, Couple stress theory for solids, International Journal of Solids and Structures 48 (2011) 2496–2510. doi:10.1016/j.ijsolstr.2011.05.002.

[6] A. Pedgaonkar, B. T. Darrall, G. F. Dargush, Mixed displacement and couple stress finite element method for anisotropic centrosymmetric materials, European Journal of Mechanics - A/Solids 85 (2021) 104074. doi:10.1016/j.euromechsol.2020.104074.

[7] D. J. Allman, A compatible triangular element including vertex rotations for plane elasticity analysis, Computers & Structures 19 (1984) 1–8. doi:10.1016/0045-7949(84)90197-4.

[8] D. Boutagouga, A review on membrane finite elements with drilling degree of freedom, Archives of Computational Methods in Engineering (2020). doi:10.1007/s11831-020-09489-z.

[9] T. L. Chang, C.-L. Lee, A. J. Carr, R. P. Dhakal, Numerical evaluations of a novel membrane element in response history analysis of reinforced concrete shear walls, Engineering Structures 220 (2020) 110760. doi:10.1016/j.engstruct.2020.110760.

[10] M. A. Khorshidi, The material length scale parameter used in couple stress theories is not a material constant, International Journal of Engineering Science 133 (2018) 15–25. doi:10.1016/j.ijengsci.2018.08.005.

[11] G. F. Dargush, G. Apostolakis, A. R. Hadjesfandiari, Two- and three-dimensional size-dependent couple stress response using a displacement-based variational method, European Journal of Mechanics - A/Solids 88 (2021) 104268. doi:10.1016/j.euromechsol.2021.104268.

[12] B. T. Darrall, G. F. Dargush, A. R. Hadjesfandiari, Finite element lagrange multiplier formulation for size-dependent skew-symmetric couple-stress planar elasticity, Acta Mechanica 225 (2013) 195–212. doi:10.1007/s00707-013-0944-9.

[13] G. Deng, G. F. Dargush, Mixed lagrangian formulation for size-dependent couple stress elastodynamic response, Acta Mechanica 227 (2016) 3451–3473. doi:10.1007/s00707-016-1644-z.

[14] A. R. Hadjesfandiari, G. F. Dargush, Couple stress theories: Theoretical underpinnings and practical aspects from a new energy perspective, 2016. `arXiv:1611.10249v1`.

[15] T. L. Chang, C.-L. Lee, A. J. Carr, R. P. Dhakal, S. Pampanin, A new drilling quadrilateral membrane element with high coarse-mesh accuracy using a modified hu-washizu principle, International Journal for Numerical Methods in Engineering 119 (2019) 639–660. doi:10.1002/nme.6066.

[16] T. L. Chang, suanpan — an open source, parallel and heterogeneous finite element analysis framework, 2021. doi:10.5281/ZENODO.1285221.

[1] Link to the repository would be added after acceptance

[17] F. Yang, A. C. M. Chong, D. C. C. Lam, P. Tong, Couple stress based strain gradient theory for elasticity, International Journal of Solids and Structures 39 (2002) 2731–2743. doi:10.1016/s0020-7683(02)00152-x.

[18] O. C. Zienkiewicz, R. L. Taylor, J. Z. Zhu, The Finite Element Method: its Basis and Fundamentals, Elsevier, 2013. doi:10.1016/c2009-0-24909-9.